ROLE OF ArcB/ArcA IN THE REGULATION OF BIOFILM FORMATION IN *ESCHERICHIA COLI* IN CONJUNCTION WITH FlhD EXPRESSION

A Paper
Submitted to the Graduate Faculty
of the
North Dakota State University
of Agriculture, and Applied Science

By

Laura Christine Nessa

In Partial Fulfillment
for the Degree of
MASTER OF SCIENCE

Major Department:
Veterinary and Microbiological Sciences

March 2014

Fargo, North Dakota

North Dakota State University
Graduate School

ROLE OF ArcB/ArcA IN THE REGULATION OF BIOFILM FORMATION IN *ESCHERICHIA COLI* IN CONJUNCTION WITH FlhD EXPRESSION

By

Laura Christine Nessa

The Supervisory Committee certifies that this ***disquisition*** complies with North Dakota State University's regulations and meets the accepted standards for the degree of

MASTER OF SCIENCE

SUPERVISORY COMMITTEE:

Birgit Pruess
Chair

Penelope Gibbs

Anne Denton

Approved:

March 26, 2014
Date

Charlene Wolf-Hall
Department Chair

ABSTRACT

The two goals of this study were to identify the affect that *arcB* has on biofilm formation and to determine whether this was dependent on AckA. Acetyl phosphate is formed from acetyl-CoA during acetate metabolism and is degraded to acetate through the enzyme AckA. ArcB is the sensor kinase of the ArcB/ArcA two-component system involved in anaerobic metabolism [1]. Another important factor is the FlhD/FlhC global transcriptional regulator complex involved in regulating motility. The overall conclusion indicates acetyl phosphate has an effect on *arcB* only when both genes are nonfunctional as demonstrated by a lack of biofilm, increased motility, and increased *flhD* expression.

To test the hypothesis, several experiments were performed including scanning electron microscopy (SEM), growth curves, motility assays, and a ß-galactosidase assay measuring *flhD* expression. The tests were performed using a parent *Escherichia coli* K-12 strain (AJW678) and mutants in *ackA, arcB*, and an *ackA arcB* double mutant.

ACKNOWLEDGEMENT

I would like to thank my committee chair Dr. Birgit Prüß whose continual encouragement, patience, and support helped me to achieve this momentous accomplishment. I thoroughly value and cherish the learning experiences and opportunities that I have been provided. I would like to thank my committee members, Dr. Penelope Gibbs and Dr. Anne Denton, for their insight and guidance. I would also like to extend my gratitude towards Dr. Shelley Horne for her technical expertise and assistance during my research. Additionally, I would like to thank Jayma Moore for processing the samples for electron microscopy imaging. Lastly, I would like to thank my parents for their never-ending encouragement and my fiancé Elliott Welker, for his great patience and encouragement.

The work is funded by the parent grant 1R15AI089403-01A1 and the supplemental grant 1R15AI089403-01S1 from the NIH.

TABLE OF CONTENTS

LIST OF TABLES

LIST OF FIGURES

LITERATURE REVIEW

Escherichia spp. consists of Gram-negative, facultative anaerobic organisms that are rod-shaped and sometimes motile. *Escherichia coli* was initially isolated in 1885 by Theodor Escherich from the feces of a child and determined to be an organism in the intestines of healthy individuals [2]. Most strains of *E. coli* are essentially harmless inhabitants of the intestinal tract, however, there are several strains of *E. coli* that cause serious infections [3]. Pathogenic *E. coli* includes Shiga toxin-producing *E. coli*, Enterotoxigenic *E. coli*, Enteropathogenic *E. coli*, Enteroaggregative *E. coli*, Uropathogenic *E. coli* and Diffusely adherent *E. coli* [3]. Shiga-toxin producing *E. coli* is responsible for numerous foodborne outbreaks throughout the United States [3]. As previously studied, pathogenic *E. coli* may have been derived from non-pathogenic commensal *E. coli* [4].

The natural reservoir of *E. coli* is the intestinal tract of mammals and the bacteria is transmitted via fecal-oral route [5]. *E. coli* can also be found in soil and water as a result of fecal contamination [5]. Many *E. coli* strains also have the ability to form complex communities called biofilms composed of bacteria surrounding themselves in extra-cellular polymeric substance (EPS). EPS forms a glue-like slime layer allowing for greater attachment to the surface [6, 7]. Biofilms can form on inanimate surfaces such as medical implants or food processing equipment and inside living animal tissues [6, 7]. Biofilms are present in most bacterial infections due to the ability of the bacteria within the biofilms to resist antibiotics and remain protected from environmental stressors [6, 7]. Gene expression before and during biofilm formation is of particular interest to those researching medical preventions and treatments. During the planktonic stage, bacteria are open to phage infection, antimicrobials, and other harmful conditions, which explains why most bacterial infections involve biofilms [6]. Biofilms can be found in dental

implants, prosthetic heart valves, contact lenses, urinary catheters, and orthopedic implants among others [6].

Significance of biofilms

Common Biofilm-associated problems

Biofilms are ubiquitous in nature with a variety of organisms surviving within these complex communities. Biofilms can also form inside the human body leading to severe infections. These infections can occur in the eye, urinary tract, on dental surfaces, and can include device-related infections [6-8]. Table 1 provides examples of biofilm-associated diseases, some of which are detailed below.

Table 1. Common biofilm-associated infections

Medical situation	**Implication**	**Bacteria**
Urinary catheters	Long-term use provides the time required for biofilms to grow	Uropathogenic *E. coli*
Cystic Fibrosis pneumonia	The mucus buildup in the lungs from cystic fibrosis provides an ideal environment for biofilms	*Pseudomonas aeruginosa*
Artificial Heart Valve	Can grow on the heart valve or in the surrounding tissues	*Staphylococcus epidermidis* *Staphylococcus aureus*
Nosocomial Infections	Possibly due to poor cleaning in the hospital or biofilms growing in pipes and air filters	*Pseudomonas aeruginosa* *Cronobacter sakazakii* *Staphylococcus aureus*
Dental Plaque	Favorable conditions within the mouth allow for biofilm growth	*Streptococcus mitis* *Streptococcus mutans* *Actinomyces viscosus*

Nosocomial infections

Urinary catheters are typically made up of latex or silicone and can be used for months at a time [7, 9]. The biofilms can form on both the inner or outer surface and typically affect 10-50% of those using short-term catheters and almost all of those using long-term catheters [7, 9]. Biofilm growth was most dependent on the hydrophobicity of the surface of the catheter and also of the pH of the urine [9]. Researchers have investigated several materials to prevent infections; including antibiotics in the catheters and different coatings but to date no one material has prevented infections in humans [9, 10].

Biofilms can grow on the device or the surrounding tissues causing endocarditis [6]. Common bacteria found on the skin (*S. epidermidis* and *S. aureus*) can lead to infections after surgery [6, 7]. Locations involving swelling and tissue damage have a greater propensity towards infection since fibrin and platelets build up around the device [6, 7]. Device-related infections are difficult to treat especially those involving biofilms. Biofilms are notoriously difficult to remove especially with antibiotics alone; coatings may be the future in preventing infections.
Biofilms play an important role in nosocomial infections including methicillin *Staphylococcus aureus* (MRSA) infections, ventilator-associated pneumonia, *Clostridium difficile* infections, and urinary tract infections [11]. Biofilms are notoriously difficult to remove so it is possible to acquire an infection from poorly cleaned ventilators, air vents, and other medical instruments. Endotrachael tubes provide an ideal environment for biofilms to form since the tube remains in a warm and dry environment for long periods of time [12]. Bacterial within biofilms are able to resist antibiotics and several different cleaning methods including shearing and scraping. Nosocomial infections remain a persistent problem of which further research needs to take place.

Each type of infection is different so addressing a common source may be the key to solving the problem.

Effect of biofilms in the food safety industry

Biofilm formation is also a problem in the food industry. Foodborne outbreaks and diseases cause numerous illnesses every year leading to billions in health care and production costs. Foodborne outbreaks can involve single planktonic cells or increasingly, biofilms. As mentioned previously, biofilms are notoriously difficult to remove especially on metal food processing surfaces and other food contact areas. Biofilms are impervious to many antimicrobials, shearing forces, and cleaners making it even more difficult to prevent cross-contamination. A variety of species form biofilms including *Salmonella enterica* on lettuce and cabbage, *Listeria monocytogenes* and *Bacillus cereus* on metal processing equipment [13]. The constant flow of a food product on a conveyor belt for example may provide nutrients for bacteria growing within a biofilm. Typically stainless steel, glass, rubber, and polyurethane are the materials used in food processing equipment, all of which can provide an ideal surface for biofilm growth. The ability of bacteria to form biofilms on processing equipment can cause major contamination in the food products especially when the bacteria disperse.

The ability of bacteria within biofilms to survive changes in pH, osmolarity, and temperature have presented many challenges to those involved in the food safety industry. The food industry has taken many measures to prevent biofilm contamination including regular cleaning to prevent irreversible attachment, antimicrobial coatings, and antimicrobial cleaners [13]. Currently the food industry uses a standard cleaning procedure which involves dry cleaning (scraping, sweeping etc.), rinsing with very hot water, addition of special detergents including hydrogen peroxide and peracetic acid, the addition of quaternary ammonium sanitizers, and the

use of testing to make certain that the biofilms have been removed [14]. Current research performed by the U.S. Department of Agriculture-Agricultural Research Service has indicated that adding a strong electronegative charge can reduce both planktonic and biofilm contamination [14]. The negative charge is added by placing the equipment in an acid bath and adding an electric charge [14]. Biofilms have a net negative charge so adding an even stronger negative charge will repel the biofilm growth. This is only the tip of the iceberg of biofilm prevention techniques.

Biofilm-dependent applications

Even though biofilms can lead to severe disease, not all biofilms are harmful. Biofilms can be used in bioremediation and wastewater treatment. Bioremediation is an emerging trend to solve environmental pollution using microorganisms. Using biofilms is potentially more efficient than using planktonic bacteria, since bacteria within biofilms are able to withstand a larger variety of conditions. Biofilms offer greater protection and adaptation of the bacteria during stressful times allowing for more successful bioremediation [15].

Of great interest is the ability of certain bacteria to degrade hydrocarbons, especially those present in oil. *Pseudomonas spp.* for example are able to use crude oil as an energy source. The bacteria are able to attach to the oil slicks and break it into smaller molecules to use for energy. Classically, dispersants have been used to clean up hydrocarbon spills, but combined with bacteria, they are able to clean up oil spills rapidly and with less potential toxicity [15, 16]. Dispersants are able to break oil slicks into more soluble droplets to be consumed by microorganisms or dissolved into the water. Dispersants can, however, be toxic to marine life and can disrupt the oceanic ecosystem. More research is needed to understand how to use

bacteria and other microorganisms to clean up pollutants without causing damage to the marine life.

Gene regulation in biofilm formation

Stages of biofilm formation

Biofilm formation requires many stages including initial attachment, irreversible attachment, maturation, and dispersal. These stages will be discussed further in Fig 1.

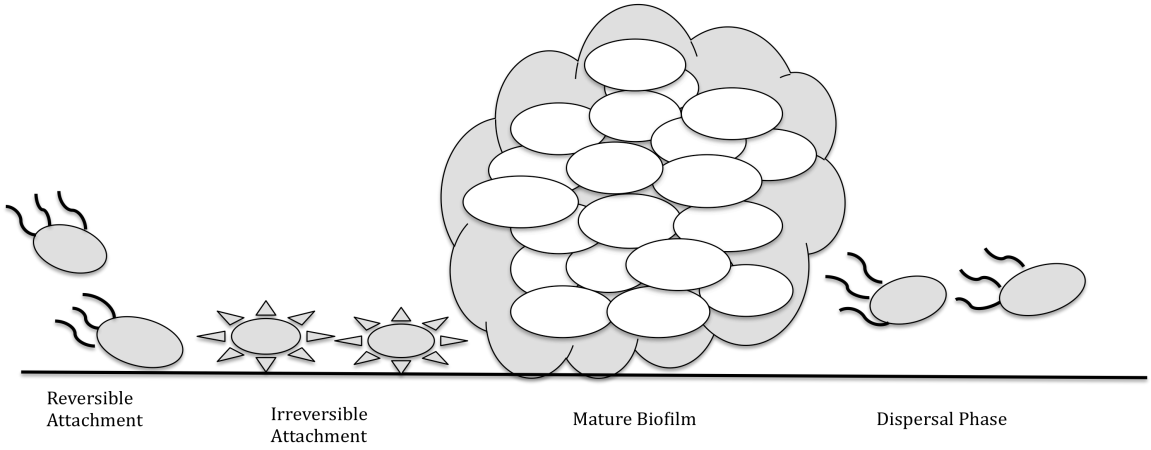

Figure 1. Stages of Biofilm Formation. During the first stage of biofilm formation, bacteria reversibly attach to the surface using flagella. In the second stage, genes encoding flagella are turned off and curli and fimbriae aid in irreversible attachment. In the third state, bacteria form a mushroom structure and are covered by an extra extracellular polymeric substance composed of a colanic acid capsule. In the final stage, bacteria may leave the biofilm once flagella gene expression is turned on. (Figure modified from [17]).

In reversible attachment, planktonic bacteria attach reversibly to a surface. Bacteria are able to leave the surface during the reversible attachment stage. Genes involved in flagella synthesis are still expressed during the reversible attachment stage. Once the bacteria are reversibly attached, they limit flagella expression and express genes for curli and fimbriae. The bacteria at this point form an irreversible attachment to the surface and once they are irreversibly attached, the bacteria form a large three-dimensional structure during the maturation stage. In

order to stay protected from the environment, bacteria produce a slime layer composed of extracellular polymeric substance (EPS) that allows the bacteria to adhere to each other. Deep within the mature biofilm the oxygen concentration is reduced and nutrients are often difficult to come by thus the bacteria change gene expression in order to survive the harsh conditions. This will be mentioned again under the *arcB* section. In the dispersal phase bacteria may turn the flagella genes on and leave the biofilm [17, 18]. Although less is known about the genes expressed during the dispersal stage.

Acetate kinase (AckA)

AckA or acetate kinase is the enzyme responsible for degrading acetyl phosphate to acetate [19, 20]. The degradation of acetyl phosphate (acetyl phosphate) into acetate is an important part of central metabolism [20, 21]. Acetyl phosphate is formed by the activity of Pta, or phosphotransacetylase through the degradation of acetyl-CoA. These reactions are summarized in Fig. 2.

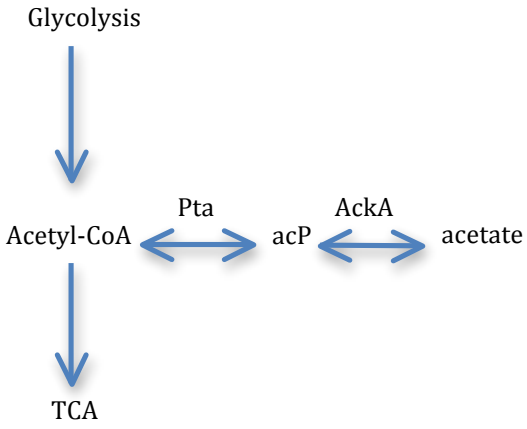

Figure 2. Acetate metabolism schematic to illustrate central metabolism. Glycolysis results in the formation of acetyl-CoA, which is degraded into acetyl phosphate by Pta. Once acetyl phosphate is formed, AckA converts it to acetate. Without AckA, acetyl phosphate acts a phosphodonor to phosphorylate response regulators.

Acetyl phosphate transmits information regarding environmental signals to the central metabolism in *E. coli* [22]. Acetyl phosphate is a high energy intermediate with an affinity to donate its phosphate to a two-component system. The two-component system is composed of a response regulator and a sensor kinase. The sensor kinase senses environmental signals and phosphorylates the response regulator where a response can take place. The acetyl phosphate can donate its phosphate to certain response regulators, such as, OmpR and PhoB [23]. OmpR is part of the EnvZ/OmpR two-component system that is involved in osmoregulation in several bacterial species [23, 24]. PhoR/PhoB is another two-component system that regulates phosphate concentration in the cell [25]. Once a signal is sensed, the sensor kinase autophosphorylates and the phosphate is transferred to the response regulator. Acetyl phosphate can act as the phosphate donor to phosphorylate the sensor kinase. In this sense, acetyl phosphate acts as a global regulator that gathers information from the environment and modulates response regulator activity.

Acetyl phosphate may also mediate the switch between reversible to irreversible attachment during biofilm formation [22]. When the expression of acetyl phosphate is low, flagella expression is increased before transition to irreversible attachment occurs [22]. The switch is thought to occur when acetyl phosphate expression is higher in the cell.

ArcB/ArcA two-component system

Another mutant that was studied for this project was a strain containing a non-functional *arcB* gene. The ArcB/ArcA two-component system or anoxic redox control contains ArcB, the membrane-bound sensor kinase, that is involved in regulating the response of changes in oxygen concentrations, along with ArcA acting as the cytosolic response regulator [26]. The ArcB/ArcA

two-component system is very important to the survival of *E. coli* cells. Surviving as a facultative anaerobe can be a difficult task, and being able to survive in both high and low concentrations of oxygen requires many genes. The ArcB sensor contains three domains including a transmitter domain (His292), a receiver domain (Asp576), and a phosphotransmitter domain (His717) [1, 27]. The ArcA response regulator contains an aspartyl residue (Asp54) [27]. When the oxygen concentration decreases ArcB senses the decrease indirectly and instead senses a change in the redox potential of ubiquinone and menaquinone [28]. ArcB then autophosphorylates during a process that can also be assisted by pyruvate, lactate, and acetate [27]. The phosphate is then transferred to the ArcA aspartyl residue where there will be a response to the environmental signal. ArcA mediates the change from respiratory metabolism to fermentative metabolism by negatively regulating genes for aerobic metabolism pathways [1, 27]. This reaction can also proceed in the reverse once the bacteria are under aerobic conditions; for example ArcB dephosphorylates ArcA.

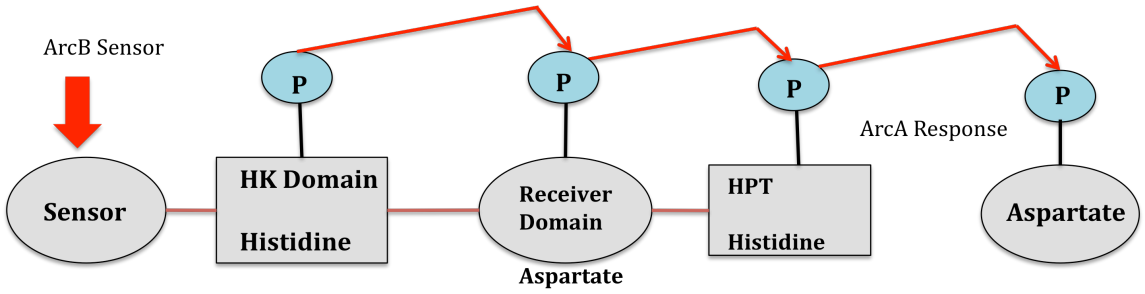

Figure 3. The ArcB/ArcA two-component system. The two-component system contains multiple phosphotransmitter domains including a histidine kinase domain, a receiver domain, and a histidine phosphotransmitter domain. The ArcA response regulator contains a typical aspartyl domain. The phosphate is transferred to the response regulator once low oxygen conditions are sensed (Figure modified from [29]).

On a biochemical level, ArcB phosphorylation occurs when there is a greater reduction potential than oxidation [30]. Quinone carriers prevent ArcB phosphorylation when the oxidation conditions occur in the cells [30]. When the cell is under anaerobic conditions the electron

carriers (ubiquinone and menaquinone) are reduced releasing disulfide bonds activating autophosphorylation [28].

ArcZ – small non-coding RNA

Another important gene involved in the ArcB/ArcA two-component system is *arcZ.* The *arcZ* gene is a small non-coding RNA involved in the binding of Hfq (an RNA chaperone protein) to positively regulate the stress-response gene *rpoS* [31]. ArcZ is a negative regulator of *rpoS* mRNA translation and has also been shown to negatively regulate FlhDC by base-pairing with the 5'UTR mRNA [31]. FlhDC is a master regulator of flagella and will be discussed in the next section. The synthesis of flagella is regulated at the transcriptional and post-translational levels indicating that the small non-coding RNAs may be involved in the regulation [31]. In a study performed by Gottesman et al, it was found that ArcZ eliminated motility and negatively regulates FlhD and FlhC by binding to the FlhDC mRNA [31]. This occurs post-transcriptionally therefore preventing translation of the motility regulator. ArcZ is also repressed by the ArcB/ArcA two-component system once ArcA is phosphorylated by ArcB [31]. The *arcZ* expression is therefore higher under aerobic conditions while *arcB* is inhibited under aerobic conditions. Further research is needed to determine the impact of ArcZ pairing with FlhDC impacts motility.

Master motility regulator FlhDC

FlhDC is the master regulator of flagella synthesis and as mentioned previously, flagella are an important factor in both the initial and dispersal phases of biofilm formation. FlhDC regulates over 50 genes including *fliA, flgM*, and *fliC* [32, 33]. FliA and FlgM direct transcription of class III operons involved in chemotaxis and filament construction [32]. FliC is a class III

gene and encodes for flagellin, which forms the filament of the flagellum [32]. These genes function to build the basal body, hook, and filament, which forms the structure of flagella [32]. Previous studies performed in our lab have shown that the expression of FlhC reduced biofilm formation and the cell division rate of *E. coli* O157:H7 [34]. Besides regulating flagella synthesis, FlhDC has also been linked to the regulation of anaerobic respiration [35]. This may indicate that FlhDC is involved in regulating the switch from aerobic to anaerobic growth [36]. As discussed earlier, ArcB/ArcA two-component system is involved in the switch from aerobic to anaerobic respiration and potentially regulates *flhD* expression [31]. The osmoregulator, EnvZ/OmpR, and colanic acid regulator RcsCDB also regulate the *flhD* operon. Both of these two component systems negatively regulate *flhD* [23, 37, 38].

RATIONALE

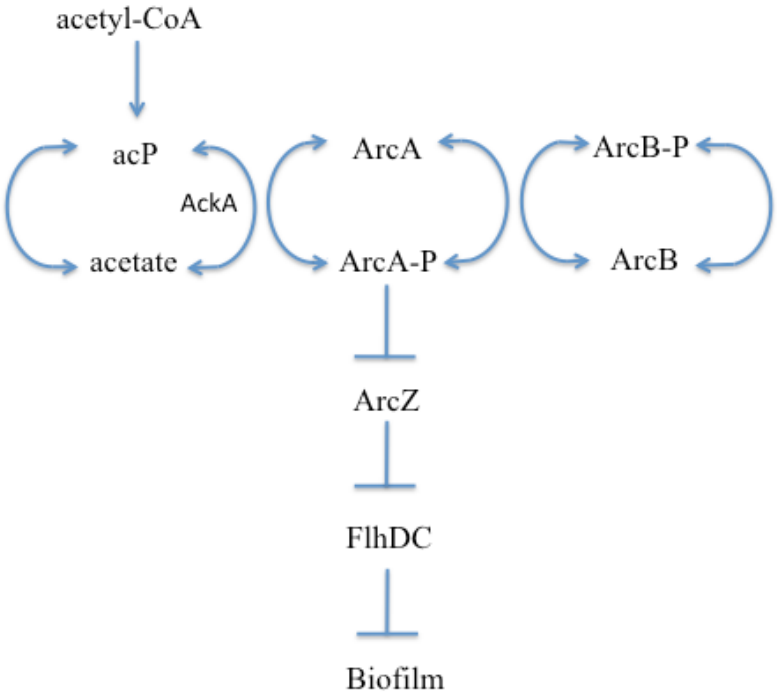

Figure 4. Rationale of study. The hypothesis of the experiments is that ArcB/ArcA has a role in biofilm formation possibly involving acetyl phosphate and through the negative regulation of *flhD*.

The question has been raised whether ArcB has a role in the formation of biofilms. Several experiments were performed to facilitate further understanding of the role it plays in biofilm formation. It is plausible that since ArcB is the sensor kinase part of a two-component system that responds to changes in oxygen concentration there would be an effect on biofilm formation. Anaerobic conditions are found deep within biofilms so survival could be dependent on an intact ArcB/ArcA system among other two-component systems. In order to determine whether there was a correlation to biofilm formation, a strain containing a nonfunctional *arcB* gene was subjected to scanning electron microscopy, motility assays, a growth curve, and a ß-galactosidase assay measuring *flhD* expression.

Another aim was to determine what effect an accumulation of acetyl phosphate would have on the ArcB biofilm formation. To measure the effect, one strain containing nonfunctional *ackA* and *arcB* genes was examined using scanning electron microscopy (SEM) and a ß-galactosidase assay quantifying biofilm amounts. The overall results indicated that biofilm formation changes only when both *ackA* and *arcB* are nonfunctional.

MATERIALS AND METHODS

Bacterial strains

Dr. Alan J. Wolfe of Loyola University Chicago (Maywood, IL) provided the strains used in this experiment. The *ackA*, *arcB*, and *ackA arcB* double mutants were compared to the AJW678 wild-type strain.

Table 2. Bacterial strains

	Strains[1]		
		Relevant genotypes	**Reference**
	CP875	*thi-1 thr-1*(am) *leuB6 metF159*(Am) *rpsL136 ΔlaxX74 λlacY*	Pruess et al., 1994
1	AJW678	*thi-1 thr-1*(am) *leuB6 metF159*(Am) *rpsL136 ΔlaxX74*	Kumari et al. 2000
2	CP891	CP875 *ackA*::Tn*phoA*'-2 tet	Pruess et al., 1994
	JJ5536-1	BW25311 *arcB*::*Tn*5	CGSC[2]
3	BP1283	AJW678 *arcB*::*Tn*5	This study
4	BP1329	AJW678 *ackA*Tn*phoA arcB*::*Tn*5	This Study
	CP992	OW1 D(*lac*)58 *flhD*::*lacZ*	Shin and Park, 1995
	BP509	MC1000 *flhD*::*lacZ*	This study
5	BP1566	AJW678 *flhD*::*lacZ*	This Study
6	BP1567	AJW678 *ackA::TnphoA'-2 tet - flhD::lacZ*	This Study
7	BP1568	AJW678 *arcB*::*Tn*5- *flhD::lacZ*	This Study
8	BP1569	AJW678 *ackA::TnphoA'-2 tet arcB::Tn5- flhD::lacZ*	This Study

[1]Strains that were used in the physiological experiments are numbered consecutively. Strains 1 through 4 were used for the electron microscopy, growth curve, and motility plates. They also served as recipient strains for the P1 transductions. BP509 is the donor strain for the P1 transduction. Strains 5 through 8 were used for the gene expression experiment.
[2]CGSC, Coli Genetic Stock Center

Growth conditions

Bacterial strains were stored at -80˚C in 80% glycerol. For experimental use, bacterial strains were streaked onto Luria Bertani (LB, 1% tryptone, 0.5% yeast extract, 0.5% NaCl, 1.5% agar) plates and incubated at 37˚C overnight. The cultures were streaked for isolation on the LB plate with one colony chosen to inoculate overnight culture. The colony was placed in liquid LB broth and grown at 37˚C overnight and aerated at 150 rpm.

Electron microscopy of bacterial biofilms

Growth of biofilms

A 12 mm glass coverslip (Assistent, Sondheim, Germany) was placed into the six-well plate prior to inoculation of all four strains allowing the biofilms to grow on the surface of the coverslip. From the overnight culture, the AJW678, *ackA, arcB*, and *ackA arcB* strains were diluted 1:100 in 4 ml of LB broth and placed into one well of a six-well plate. The Strains were incubated at 32˚C for 48 hours unaerated. After 48 hours, each well was washed twice with 4 ml phosphate buffered saline (PBS). The coverslips were removed from each well for further preparation.

Preparation of biofilms for SEM

The biofilm containing glass cover slips were placed into a vial containing 2 ml of 2.5% glutaraldehyde fixative in 0.1 mol l^{-1} sodium phosphate buffer (Tousimis Research Corporation, Rockville, MD). Bacteria were fixed for 2 hours at 4˚C. The samples were dehydrated with a graded alcohol series treatment and then critical point dried. For the graded alcohol series, biofilm samples were treated for 15 minutes each in 30%, 50%, 70%, and 90% ethanol and finally with 100% ethanol for 15 minutes twice [21, 39]. The samples also required critical

drying using liquid carbon dioxide using an Autosamdri-810 critical point drier (Tousimis Research Corporation, Rockville MD). Following critical point drying, the glass coverslips were mounted on aluminum mounts with adhesive silver paint and coated with gold-palladium using Balzers SCK 030 sputter coater (Balzers Union Ltd., Liechtenstein) [39].

SEM images

Images were obtained using a JEOL JSM-6490LV scanning electron microscope (JEOL USA, Peabody MA). The strains were viewed at 1,000X, 3,000X, and 6,500X magnification. This procedure was repeated three times producing approximately 36 images per strain. One representative image per strain is presented.

Growth curve

A growth curve was produced using the same four strains as were used in the SEM experiment were plated from freezer stock. From the overnight cultures, 1 ml cultures were produced in cuvettes containing LB broth and covered with parafilm (American National Can Co., Greenwich CT) at an inoculation of 1:100 in LB broth. Cultures were incubated at 32˚C. The OD_{600} was read hourly for 6 hours and once per day for seven days using an Eppendorf BioPhotometer 6131 (Eppendorf, Hamburg Germany). The growth curve was measured by observing the shape of the curve and looking at how the *ackA, arcB*, and, *ackA arcB* compare to the AJW678 strain.

Motility characterization

Motility of the strains was also analyzed through swarm data collection. Motility agar plates were made from motility agar (1% tryptone, 0.5% NaCl, and 0.3% Bacto agar) on petri dishes (150 mm × 15 mm). Bacteria were grown on fresh LB plates daily and used for

inoculation of the motility agar plates. Single colonies were spotted into the center of the plates, which were then incubated at 25˚C, 32˚C, and 37˚C. The procedure was performed in triplicate with the four strains from the previous experiments at each temperature. The diameter in millimeters was measured every three hours for approximately 30 hours. The swarm rate was determined across 30 hours (measured in mm/h using average and standard deviation.)

P1 transduction

The P1 phage was used for transduction of the *flhD*::*lacZ* from CP992 into the four strains used in the previous experiments through MC1000 [40].

Preparation of the phage lysate from the donor strain

From overnight cultures, 50 µl of the MC1000 *flhD*::*lacZ* donor strain was added to 5 ml of LB broth, supplemented with 0.2% glucose and 5 mM $CaCl_2$. The sample was aerated for 30 minutes at 37˚C. After 30 minutes, 100 µl of a lysate was added to the tube and incubated for 2-3 hours until clearing or lysis occurred. Once lysed, 100 µl of chloroform was added and the sample was vortexed. The lysate was centrifuged at 3,000 rpm for 15 minutes. Another 100 µl of chloroform was added and the lysate was stored at 4˚C for future use.

Transduction procedure

Overnight cultures of the recipient strains were diluted to OD_{600} of 0.02-0.04 in LB broth (400 µl sample, 20 ml of LB broth,) supplemented with 0.1% glucose and 10 mM of $CaCl_2$. The samples were aerated at 37˚C until cultures reached log phase (OD_{600} 0.4-0.6). Once log phase was reached, 1 ml of cells were infected with 0, 10, 50, or 100 µl of phage lysate from the donor strain and incubated at 37˚C for 20 minutes unaerated. To the bacterial samples, 200 µl of sodium citrate was added and centrifuged at 3,000 rpm for 5-10 minutes. The pellet was

resuspended in 500 µl LB broth and 200 µl sodium citrate and incubated for 1 hour at 37˚C unaerated. The samples were centrifuged at 3,000 rpm for 5-10 minutes. The pellet was resuspended in 100 µl of sodium citrate and the samples were plated on LB agar plates, containing 50 mg/ml of X-gal (5-bromo-4-chloro-3-indolyl-β-D-galactopyranoside). For controls, 100 µl of lysate and 100 µl of uninfected cells were used.

Blue-white screening

The samples made from the transduction procedure were plated onto X-gal-containing LB plates to determine whether the *flhD::lacZ* fusion was present in the newly created strains. X-gal is used to determine whether the *lacZ* gene is functional. If transduction was successful in this case there will be white colonies with a few blue colonies. Blue colonies are indicative of a functional *lacZ* gene.

ß-galactosidase assay for *flhD* expression

The ß-galactosidase assay was used to measure *flhD* expression in biofilms of BP1566, BP1567, BP1568, and BP1569 strains, refer to table 2 for more information. A 1:100 dilution of overnight culture was added to each well of a 24-well plate. The plates were read at 96 hours and repeated six times.

Plate processing

Using the ß-galactosidase from Miller, 1972 [40] the *flhD* expression can be measured. On the day of processing, each well was washed twice with 1 ml of PBS. After washing, 1 ml of Z-buffer (0.06 M Na_2HPO_4 +7H_2O, 0.04 M NaH_2PO_4 +H_2O, 0.01 M KCl, 0.001 M $MgS0_4$ +7H_2O, 0.05 M ß-mercaptoethanol) was added to resuspend the biofilm. To determine the biomass of the biofilm, the OD_{600} was measured using the BioTek Synergy™H1 plate reader

(Winooski, VT). To measure ß-galactosidase activity, the plate was further processed with 20 µl chloroform and 10 µl 0.1% SDS (Sodium dodecyl sulfate) into each well to lyse the cells. Bacterial lysates from each well were transferred to a clean 24-well plate after the chloroform destroyed the plastic. From here, 200 µl ONPG (40 mg ortho-Nitrophenyl-β-galactoside dissolved in 10 ml Z-buffer) was added to each well. The production of ortho nitrophenol (ONP) was determined at 420 nm using the BioTek Synergy™H1 plate reader (Winooski, VT). The OD_{600} and OD_{420} were each measured per minute and the OD_{420} was divided by the O_{D600}. The rate of change in mOD_{420}/mOD_{600} /min was measured to determine the *flhD* expression of each strain. The experiment was repeated several times and the *flhD expression* was determined using the average and standard deviation.

RESULTS

SEM biofilm

SEM imaging was performed on the *ackA, arcB,* and *ackA arcB* mutant strains and was compared to the AJW678 parent strain (Fig. 5). The AJW678 parent strain displayed a thin layer of bacteria with minor three-dimensional structuring. The *arcB* mutant also displayed a thin layer of bacteria but had more three-dimensional structuring. This is in contrast to the *ackA* mutant, which produced a biofilm that contained slightly more bacteria, which were also more organized in three-dimensional structures. The *ackA arcB* double mutant produced no biofilm.

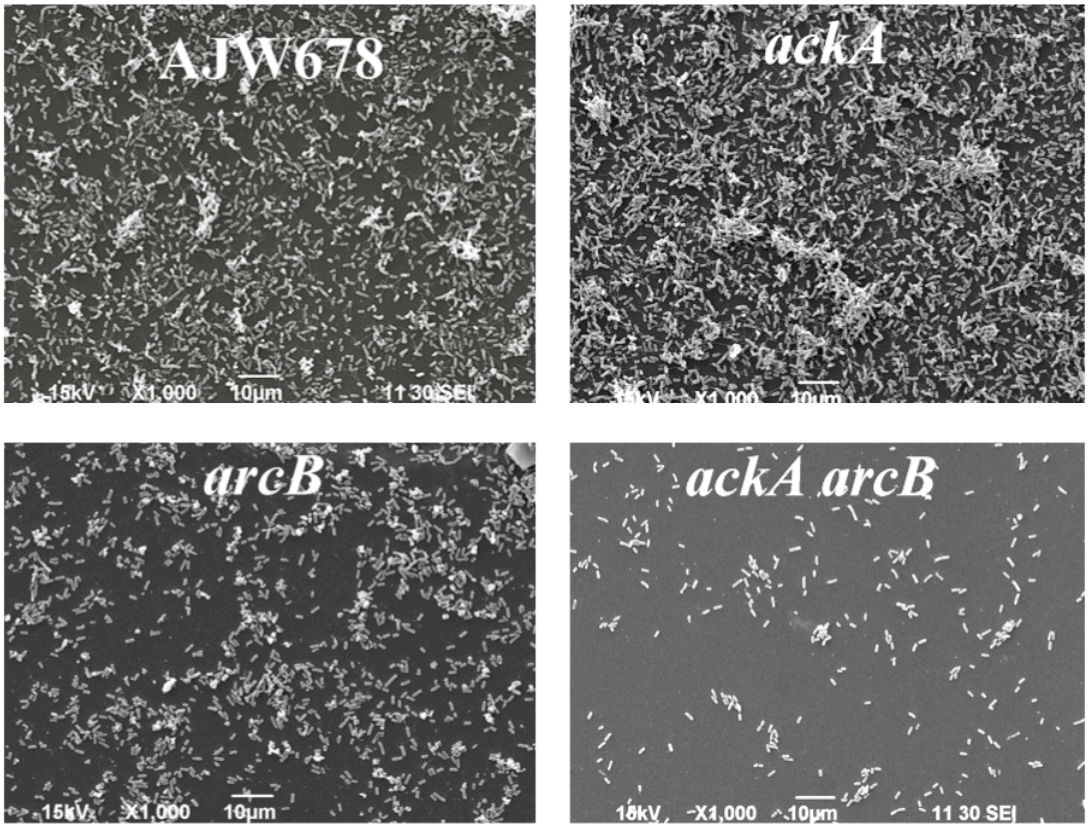

Figure 5. Scanning Electron Microscopy. SEM was used visualize biofilm formation in the *E. coli* parental strain (AJW678), and the *arcB*, *ackA*, *ackA arcB* mutants. The images are viewed at 1,000X magnification.

Growth curve

A growth curve was performed to determine whether the lack of biofilm produced by the *ackA arcB* double mutant was due to a growth deficiency (Fig. 6). The growth curves of the *ackA, arcB,* and *ackA arcB* mutants were compared to the AJW678 strain. The results indicate that although the *ackA arcB* mutant grew at a slower initial rate than AJW678 and the *arcB* mutant, it eventually caught up and surpassed the AJW678 strain. AJW678 and the *arcB* mutant strain had a similar growth pattern to one another, while the *ackA* mutant strain grew at a slower rate initially and eventually caught up to the other strains. Overall, the *ackA arcB* mutant did not have a growth deficiency that could account for poor biofilm formation.

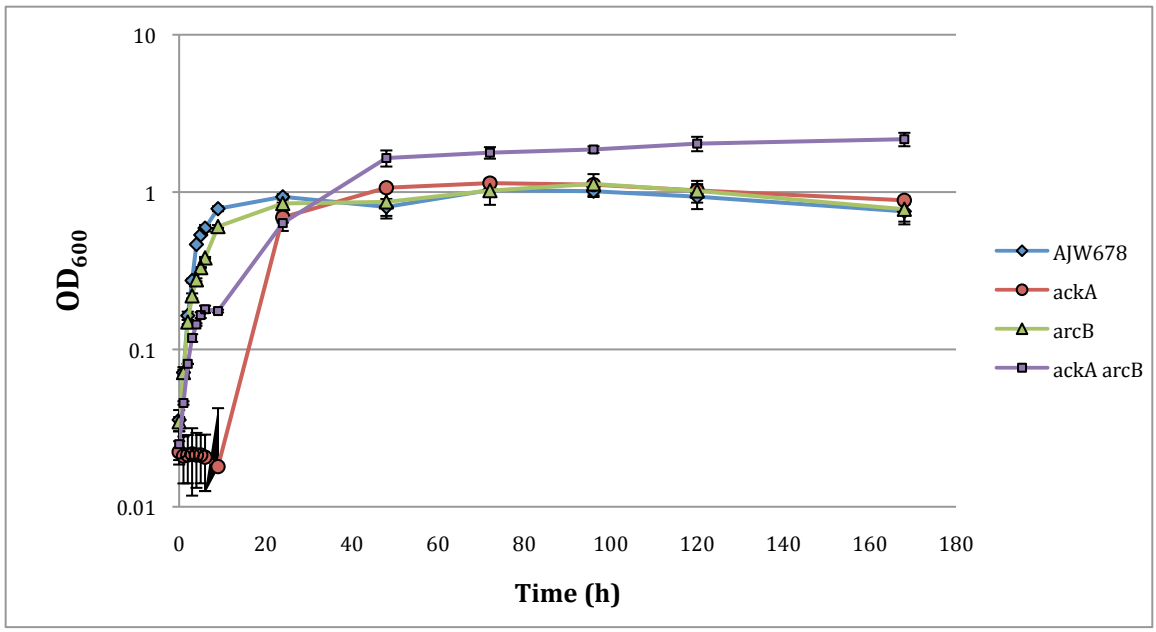

Figure 6. Growth curve analysis of AJW678, *ackA*, *arcB*, and *ackA arcB*. The experiment was performed using an Eppendorf Spectrophotometer and the strains were incubated at 32˚C for 48 hours.

Motility characterization

To investigate the relationship between biofilm and motility, motility assays were performed for the four strains at three different growth temperatures (Fig. 7). At 25˚C all four strains had a slower swarm rate. However, beginning at 32˚C the strains displayed a faster swarm rate as the temperature increased. At 37˚C the four strains had a larger swarm rate than at 32˚C. This leads to the conclusion that the swarm rate of the strains is temperature dependent. At all three growth temperatures, the *ackA arcB* double mutant swarmed at a much faster rate than any of the other strains while the *ackA* mutant swarmed the slowest. There was a more pronounced difference between the *ackA arcB* double mutant than the other strains at 37˚C. The graph also shows a plateau in the *ackA arcB* double mutant at 37˚C, which is due to the size of the plates (120mm in diameter) used in the experiment.

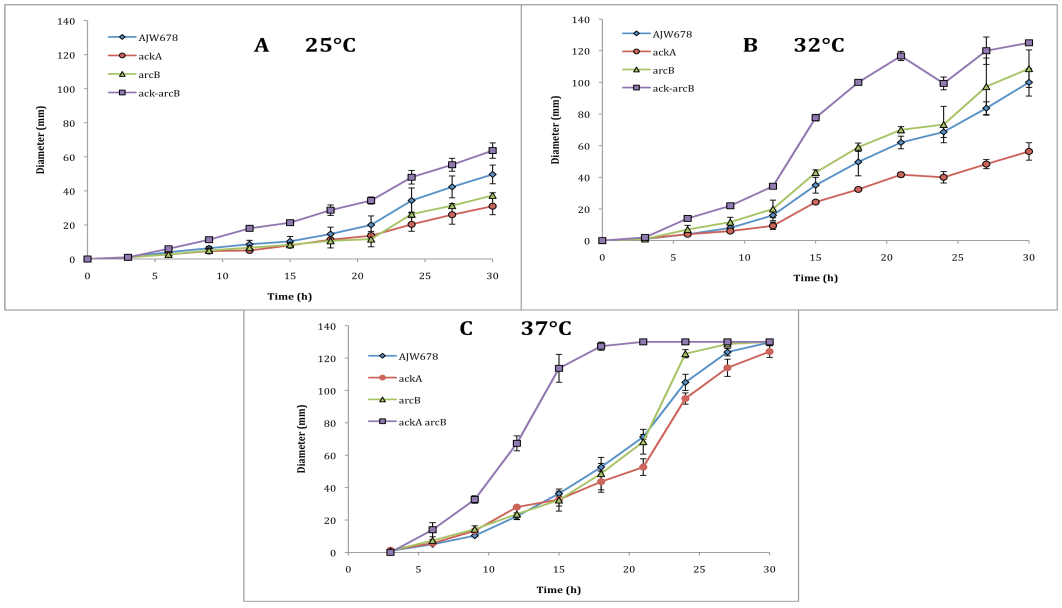

Figure 7. Swarm rates at three different temperatures. Swarm rate was measured at three different temperatures for 30 hours. The X-axis refers to the time in hours and the Y-axis refers to the diameter measurement in millimeters. Graph A—25˚C, Graph B—32˚C, and Graph C—37˚C.

ß-galactosidase assay measuring *flhD* expression

The ß-galactosidase assay was performed to measure the *flhD* expression of the experimental strains at different time points during biofilm formation (Fig. 8). As mentioned previously, *flhD* is involved in the synthesis of flagella, which is an important factor in biofilm formation. The *flhD* expression was measured in $mOD_{420}/OD_{600}/min$. The results indicate that the expression of *flhD* was slightly higher in the *ackA arcB* double mutant than in the parent and very low in the *ackA* mutant. Prior to processing the plate for the ß-galactosidase assay, the amount of biofilm was quantified using the plate reader. The biofilm quantification was used to confirm the SEM image conclusions and the motility testing results. The lack of biofilm by the *ackA arcB* double mutant was confirmed using the quantification method.

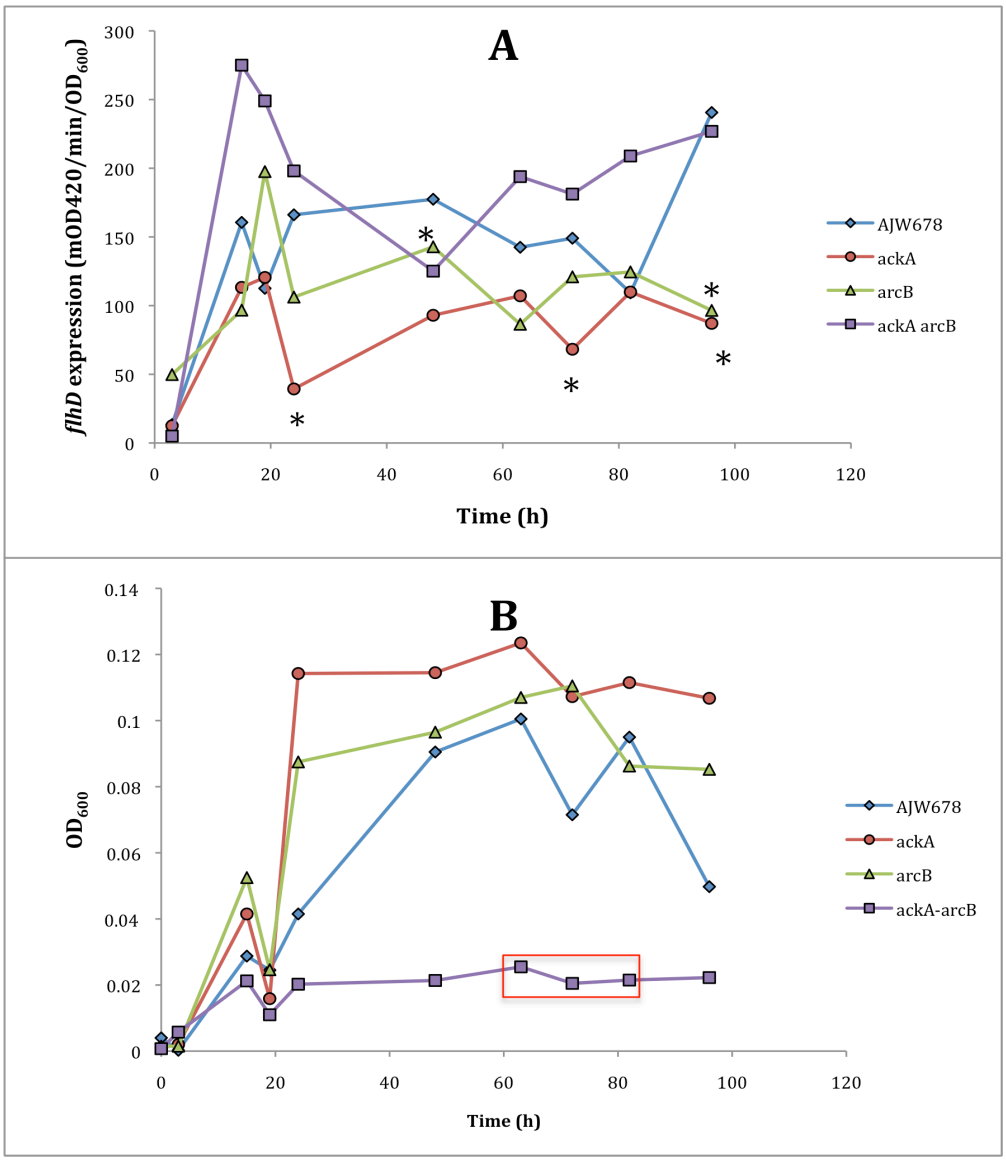

Figure 8. ß-galactosidase assay to measure *flhD* expression and biofilm quantification. The samples were incubated at 32˚C for up to 96 hours. Panel A shows the flhD expression during different time points. Panel B shows the biofilm quantification measured using the same plate. The Asterisks and red box indicate a significant difference between the samples.

DISCUSSION

The two goals of this study were to identify the affect that *arcB* has on biofilm formation and to determine whether this was dependent on AckA. The overall results showed that *ackA* and *arcB* had an effect on biofilm only when both genes were nonfunctional. This was demonstrated by the lack of biofilm in the SEM, increased motility, and increased *flhD* expression. Independently, the *arcB* mutant was very similar to that of AJW678 (wild-type) throughout all experiments and the *ackA* mutant demonstrated results similar to those of previous studies [22, 41].

Previous data has shown that the *ackA* mutant forms thick biofilms due to acetyl phosphate accumulation [22]. Therefore, this strain is able to serve as the positive control that the SEM is yielding reliable results. The SEM images show that the *ackA* mutant displayed a thin biofilm that contained slightly more bacteria with more organized three-dimensional structuring than in the AJW678 strain as depicted in figure 5. A growth curve was performed to examine the growth pattern of the four strains with the *ackA* mutant growing at a slower rate than AJW678. The four strains are described in table 2. The growth pattern has been documented previously showing slow growth in the *ackA* mutant [41]. A motility assay was performed to determine the swarm rate of the strains, refer to figure 7. The results showed that the swarm rate was temperature dependent and in particular, the *ackA* mutant swarmed slower than the other strains especially at 32˚C and could be explained in part by the slow growth of the strain [41]. A ß-galactosidase assay was performed to measure *flhD* expression during different time points, refer to figure 8. AckA, a mutant known to form thick biofilms, had low *flhD* expression rate throughout confirming the results in the motility assay. Biofilm quantification was measured using the same plate as the ß-galactosidase assay and measured biofilm formation during

different time points. The *ackA* mutant formed larger amount of biofilm after 24 hours with an optical density higher than that of the AJW678 strain.

In addition, it was hypothesized that ArcB/ArcA was among the two-component systems that might regulate biofilm through the *wza* operon that is responsible for the synthesis of colanic acid [42]. For this study, it was of particular interest to investigate the role of the ArcB/ArcA two-component system on biofilm formation in the presence and absence of AckA. The SEM results indicated, though not entirely in a consistent manner, that the *arcB* mutant displayed a thin layer of bacteria with minor three-dimensional structuring similar to that of the AJW678 strain. The *arcB* mutant displayed a very similar growth pattern and motility pattern to that of the AJW678 strain. The *flhD* expression was similar to that of the AJW678 strain but the biofilm quantification demonstrated that the *arcB* mutant had a slightly higher optical density than the AJW678 strain indicating that it may form a slightly thicker biofilm. Overall, the results of the experiments for *arcB* were very similar to that of the AJW678 strain.

A goal of the study was to determine the effect that *ackA* has on *arcB*. The SEM results showed that the *ackA arcB* double mutant formed no biofilm. This was seen on all images and was produced with a high degree of consistency. Since no biofilm was produced, a growth curve was performed to determine whether there was a growth deficiency that could account for the lack of biofilm formation in the *ackA arcB* double mutant. The results show that the *ackA arcB* double mutant was a slow grower; however it caught up and surpassed the other strains. It can be concluded that *ackA arcB* did not have a growth deficiency that could explain the lack of biofilm formation. A motility assay was utilized to measure the swarm rate of the mutants. The *ackA arcB* double mutant swarmed at a faster rate than the other strains especially when temperature was increased. This result necessitated further examination of *flhD* expression since *flhD* is

involved in motility. The results show that the *flhD* expression of the *ackA arcB* double mutant was slightly higher than in the AJW678 confirming the results of the motility assay. The biofilm amounts were also quantified and the results indicated that the *ackA arcB* double mutant had a very low optical density throughout the time points indicating that no biofilm was formed, which confirms the SEM results.

There were, however, a few problems with the ß-galactosidase assay. The chloroform destroyed the plastic in the plates, which required the transfer of the sample several times to new plates. In doing so, sample was left behind making it impossible to know how many lysed cells were left behind potentially impacting the results. A better study would be using fluorescence from a *flhD*::*gfp* fusion to examine *flhD* expression. This type of assay would not require the lysis of cells or any further processing. At the point in which *flhD* expression was to be measured a fluorescence assay was unavailable.

Table 3. Overall conclusions

	WT	*ackA*	*ackA arcB*	Correlation
Biofilm	++	+++	-	NA
Growth	++	+	++	None
Motility	++	+	+++	Inverse to biofilm
flhD	++	+	+++	Positive to motility, Inverse to biofilm

The experiments identified a potential link between *ackA* and *arcB* since biofilm formation was only impacted once both genes were nonfunctional. The reason as to why this occurred is unknown. Further investigation of *arcA* and *arcZ* and their role in biofilm formation

is needed to understand how *ackA* can affect *arcB*. Since *arcA* is part of the ArcB/ArcA two-component system it would be interesting to determine what effect a mutant in *arcA* would have on biofilm formation since acetyl phosphate may be unable to phosphorylate *arcA* independently of *arcB* [43]. ArcA has also been shown to regulate *fliA,* which is involved in motility [44]. The same study also indicated that *arcB* does not play much of role in motility so it may be worth examining motility and *flhD* expression in an *arcA* mutant [44]. The results of the motility assay performed in our lab found that *arcB* had a very similar motility pattern to that of the AJW678 strain so further examination of *arcA* is needed. ArcB/ArcA has also been shown to partially regulate *flhD* expression by repression of *arcZ,* which further indicates that there has to be a relationship between *arcB* and *arcA* that needs to be studied with respect to biofilm formation and motility.

REFERENCES

1. Pena-Sandoval, G.R. and D. Georgellis, *The ArcB sensor kinase of Escherichia coli autophosphorylates by an intramolecular reaction.* J Bacteriol, 2010. **192**(6): p. 1735-9.
2. Shulman, S.T., H.C. Friedmann, and R.H. Sims, *Theodor Escherich: the first pediatric infectious diseases physician?* Clin Infect Dis, 2007. **45**(8): p. 1025-9.
3. Anastasi, E.M., et al., *Pathogenic Escherichia coli found in sewage treatment plants and environmental waters.* Appl Environ Microbiol, 2012. **78**(16): p. 5536-41.
4. Wang, X., et al., *Serotypes, virulence factors, and antimicrobial susceptibilities of vaginal and fecal isolates of Escherichia coli from giant pandas.* Appl Environ Microbiol, 2013. **79**(17): p. 5146-50.
5. Duriez, P., et al., *Commensal Escherichia coli isolates are phylogenetically distributed among geographically distinct human populations.* Microbiology, 2001. **147**(Pt 6): p. 1671-6.
6. Zhao, G., et al., *Biofilms and Inflammation in Chronic Wounds.* Adv Wound Care (New Rochelle), 2013. **2**(7): p. 389-399.
7. Donlan, R.M., *Biofilms and device-associated infections.* Emerg Infect Dis, 2001. **7**(2): p. 277-81.
8. Loesche, W.J., *Role of Streptococcus mutans in human dental decay.* Microbiol Rev, 1986. **50**(4): p. 353-80.
9. Chen, M., Q. Yu, and H. Sun, *Novel strategies for the prevention and treatment of biofilm related infections.* Int J Mol Sci, 2013. **14**(9): p. 18488-501.
10. Hatt, J.K. and P.N. Rather, *Role of bacterial biofilms in urinary tract infections.* Curr Top Microbiol Immunol, 2008. **322**: p. 163-92.

11. Bryers, J.D., *Medical biofilms.* Biotechnol Bioeng, 2008. **100**(1): p. 1-18.

12. Gil-Perotin, S., et al., *Implications of endotracheal tube biofilm in ventilator-associated pneumonia response: a state of concept.* Crit Care, 2012. **16**(3): p. R93.

13. Sokunrotanak, S., I.K. Jahid, and S.D. Ha, *Biofilm formation in food industries: A food safety concern.* Food Control, 2013. **31**(2): p. 572-585.

14. Cramer, M., *Biofilms: Impact on the Food Industry*, in *Food Safety Magazine*2012, Stacy Atchison: Glendale, CA. p. 20-23.

15. Dasgupta, D., R. Ghosh, and T.K. Sengupta, *Biofilm-Mediated Enhanced Crude Oil Degradation by Newly Isolated Pseudomonas Species.* ISRN Biotechnology, 2013.

16. Agency, U.S.E.P. *Oil Spill Response Techniques*. 2013; Available from: http://www.epa.gov/oem/content/learning/oiltech.htm.

17. Monroe, D., *Looking for chinks in the armor of bacterial biofilms.* PLoS Biol, 2007. **5**(11): p. e307.

18. Taktikos, J., H. Stark, and V. Zaburdaev, *How the motility pattern of bacteria affects their dispersal and chemotaxis.* PLoS One, 2013. **8**(12): p. e81936.

19. Mugabi, R., et al., *The role of activated acetate intermediates in the control of biofilm amounts.* Webmedcentral, 2012. **3**(7).

20. Brown, T.D., M.C. Jones-Mortimer, and H.L. Kornberg, *The enzymic interconversion of acetate and acetyl-coenzyme A in Escherichia coli.* J Gen Microbiol, 1977. **102**(2): p. 327-36.

21. Prüß, B.M., et al., *Environmental and genetic factors that contribute to Escherichia coli K-12 biofilm formation.* Arch Microbiol, 2010. **192**(9): p. 715-28.

22. Wolfe, A.J., et al., *Evidence that acetyl phosphate functions as a global signal during biofilm development.* Mol Microbiol, 2003. **48**(4): p. 977-88.

23. Samanta, P., et al., *OmpR and RcsB abolish temporal and spatial changes in expression of flhD in Escherichia coli Biofilm.* BMC Microbiol, 2013. **13**(1): p. 182.

24. Rentschler, A.E., et al., *OmpR regulation of the uropathogenic Escherichia coli fimB gene in an acidic/high osmolality environment.* Microbiology, 2013. **159**(Pt 2): p. 316-27.

25. Marzan, L.W. and K. Shimizu, *Metabolic regulation of Escherichia coli and its phoB and phoR genes knockout mutants under phosphate and nitrogen limitations as well as at acidic condition.* Microb Cell Fact, 2011. **10**: p. 39.

26. Alvarez, A.F., C. Rodriguez, and D. Georgellis, *Ubiquinone and menaquinone electron carriers represent the yin and yang in the redox regulation of the ArcB sensor kinase.* J Bacteriol, 2013. **195**(13): p. 3054-61.

27. Nizam, S.A., J. Zhu, P. Y. Ho, K. Shimizu, *Effects of arcA and arcB genes knockout on the metabolism in Escherichia coli under aerobic condition.* Biochemical Engineering Journal, 2009. **44**(2-3): p. 240-250.

28. Lassak, J., et al., *ArcS, the cognate sensor kinase in an atypical Arc system of Shewanella oneidensis MR-1.* Appl Environ Microbiol, 2010. **76**(10): p. 3263-74.

29. Attwood, P.V., *P-N bond protein phosphatases.* Biochim Biophys Acta, 2013. **1834**(1): p. 470-8.

30. Sharma, P., et al., *Kinase activity of ArcB from Escherichia coli is subject to regulation by both ubiquinone and demethylmenaquinone.* PLoS One, 2013. **8**(10): p. e75412.

31. De Lay, N. and S. Gottesman, *A complex network of small non-coding RNAs regulate motility in Escherichia coli.* Mol Microbiol, 2012. **86**(3): p. 524-38.

32. Tominaga, A., R. Lan, and P.R. Reeves, *Evolutionary changes of the flhDC flagellar master operon in Shigella strains.* J Bacteriol, 2005. **187**(12): p. 4295-302.

33. Ding, L., et al., *Functional characterization of FlgM in the regulation of flagellar synthesis and motility in Yersinia pseudotuberculosis.* Microbiology, 2009. **155**(Pt 6): p. 1890-900.

34. Sule, P., et al., *Regulation of cell division, biofilm formation, and virulence by FlhC in Escherichia coli O157:H7 grown on meat.* Appl Environ Microbiol, 2011. **77**(11): p. 3653-62.

35. Prüß, B.M., et al., *FlhD/FlhC is a regulator of anaerobic respiration and the Entner-Doudoroff pathway through induction of the methyl-accepting chemotaxis protein Aer.* J Bacteriol, 2003. **185**(2): p. 534-43.

36. Wolfe, A.J., *The acetate switch.* Microbiol Mol Biol Rev, 2005. **69**(1): p. 12-50.

37. Girgis, H.S., et al., *A comprehensive genetic characterization of bacterial motility.* PLoS Genet, 2007. **3**(9): p. 1644-60.

38. Francez-Charlot, A., et al., *RcsCDB His-Asp phosphorelay system negatively regulates the flhDC operon in Escherichia coli.* Mol Microbiol, 2003. **49**(3): p. 823-32.

39. Sule, P., et al., *A combination of assays reveals biomass differences in biofilms formed by Escherichia coli mutants.* Lett Appl Microbiol, 2009. **49**(3): p. 299-304.

40. Miller, J.H., *Experiments in molecular genetics.* Cold Spring Harbor Laboratory, 1972: p. 352-355.

41. Prüß, B.M. and A.J. Wolfe, *Regulation of acetyl phosphate synthesis and degradation, and the control of flagellar expression in Escherichia coli.* Mol Microbiol, 1994. **12**(6): p. 973-84.

42. Denton, A.M., et al., *Relating gene expression data on two-component systems to functional annotations in Escherichia coli.* BMC Bioinformatics, 2008. **9**: p. 294.

43. Liu, X., et al., *Evidence against the physiological role of acetyl phosphate in the phosphorylation of the ArcA response regulator in Escherichia coli.* J Microbiol, 2009. **47**(5): p. 657-62.

44. Kato, Y., et al., *Effect of the arcA mutation on the expression of flagella genes in Escherichia coli.* Biosci Biotechnol Biochem, 2007. **71**(1): p. 77-83.